

Chapter 5

Flip-Chip Light-Emitting-Diodes with Geometric Sapphire Shaping Structure (SSFC-LEDs)

5-1 Fabrication of SSFC-LEDs

5-1.1 Process procedure

The GaN LED structure with dominant wavelength at 460nm used in this study is grown by metal-organic chemical vapor deposition (MOCVD) on c-plane sapphire substrates. The LED structure consists of a 2- μm -thick undoped GaN layer, a 2- μm -thick highly conductive n-type GaN layer, a 0.2- μm -thick InGaN/GaN MQW, a 0.2- μm -thick p-type GaN layer and n InGaN/GaN short period super-lattice (SPS) tunneling contact layers for indium-tin-oxide (ITO).




Figure 5-1 shows the fabrication steps of flip-chip GaN LEDs with geometric sapphire shaping structure (GaN SSFC-LEDs). First, the SiO_2 film with size of $1000 \mu\text{m} \times 1000 \mu\text{m}$ is deposited onto the backside of sapphire substrate by plasma enhance chemical vapor deposition and defined using standard photolithography to serve as the wet etching hard mask. Avoiding damaging the epitaxial layer, the SiO_2 film is also deposited on the epitaxial layer as the sheathing. The sapphire substrate is then immersed into a $\text{H}_2\text{SO}_4:\text{H}_3\text{PO}_4$ (3:1) solution at an etching temperature of 330°C for 70 minutes. The sapphire wet etching rate is about $1.4 \mu\text{m}/\text{minute}$ in this sturdy and can be related to the H_3PO_4 composition and the etching temperature [24]. After finishing the sapphire shaping process, top-emitting LEDs with a size of $1000 \mu\text{m} \times 1000 \mu\text{m}$ are fabricated using standard photolithography process which are aligned with the backside sapphire shaping pattern and are partially etched

using an inductively coupled plasma etcher to expose an n-GaN layer for electrode formation. A indium tin oxide (250nm) is deposited on p-GaN layer as the transparent conductive layer. The samples are then annealed at 500 °C for 10 minutes in air. The Cr/Pt/Au (50 nm/50 nm/2500 nm) metals are deposited for the p- and n-contact pads. After conventional LEDs processes, the processed LED wafer is subjected to the laser scribed and broken into 1000 $\mu\text{m} \times 1000 \mu\text{m}$ chips.

As for the silicon sub-mount preparation, the Ti/Al (500 Å /2000 Å) metals are deposited onto the silicon sub-mount as a mirror. Secondly, the SiO₂ film of 800 Å is deposited onto it as a passivation. The Au metal of 2 μm is deposited for n and p bonding pad. The silicon sub-mount is subjected to stud bump process. Finally, the LED chips with oblique sapphire shaping sidewall are flip-chip bonded on silicon sub-mount using Panasonic ultra sonic flip chip bonder for electrical and optical measurement. Figure 5-2 shows the schematic drawing of the GaN SSFC-LEDs and a sketch indicating light may be extracted from the oblique sapphire sidewall.

5-1.2 SEM images and photomicrographs of SSFC-LEDs and conventional FC-LEDs (CFC-LEDs)

The crystallography facets are (1-102), (1-106) and (11-25) plane against the (0001) c-axis [25] and their angles against the (0001) c-axis are 60°, 30° and 50° respectively, as shown in figure 5-3 (b)~(d). In this study, the sapphire is etched for 70 minutes via the etching rate about 1.4 $\mu\text{m}/\text{minute}$ and etching depth is about 100 μm as shown in figure 5-3 (a). Furthermore, the etching structures are all V-grooves. The V-sharp structure can be used to form a cleaving line to break the thick (~450 μm) sapphire substrate. The SEM

images of CFC-LEDs and SSFC-LEDs are shown in figure 5-4. The sapphire shaping area and greatly thick windows layer are obviously observed on the SSFC-LED structure compared with the CFC-LED. The oblique sapphire geometry improves light extraction by reducing totally internally reflected (TIR) photons from the sidewall interfaces, allowing them to escape through the oblique sidewall. In addition, thicker sapphire windows layer offers significant advantages over conventional thin sapphire window layer structure by facilitating light emission from the edges of the chip. These two processes provide the SSFC-LED device with a significant reduction in photon path length for extraction compared to a conventional chip. Such benefits are shown in the photomicrographs figure 5-5 (a) CFC-LED and (b) SSFC-LED. Note that light appears to radiate evenly from the thicker windows layer and oblique sidewall of the SSFC-LED (b) as compared with that of CFC-LED (a), indicating that light extraction efficiency can be improved due to the oblique sapphire geometry and thicker window layer.

5-2 Characteristics of SSFC-LEDs

5-2.1 L-I-V measurement and far-field pattern

The LED chips are packaged into TO can without epoxy resin for the subsequent measurement. The corresponding I-V characteristics of SSFC-LEDs and CFC-LEDs are measured respectively as shown in figure 5-6. It is found that the I-V curve of SSFC-LEDs exhibits a normal p-n diode behavior with a forward voltage (@350mA) of 3.5 V, indicating that high temperature sapphire wet etching process dose not appear to adversely affect I-V characteristics of these devices.

Figure 5-7 shows the light output power and wall plug efficiency as a

function of injection current for $\lambda_p \sim 460$ nm devices of SSFC-LEDs and CFC-LEDs. It is clearly observed that the light output powers of the SSFC-LEDs are larger than those of the CFC-LEDs. Under 350 mA current injections, it is found that the enhancement of light output powers of the SSFC-LEDs and CFC-LEDs can be significantly raised from 150 mW to 234 mW and the wall plug efficiency can be increased from 12.26% to 18.98%. We note that bare SSFC-LEDs (without encapsulating an epoxy lens) exhibits 55% light extraction efficiency enhancement under 350 current injection compared to the CFC-LEDs. It is indicated that the geometric sapphire sidewall reduces the total internal reflection and improves the probability of photons escaping from semiconductor to air. Furthermore, thicker sapphire window layer offers significant advantages over conventional thin sapphire window layer structure by facilitating light emission from the edges of the chip.

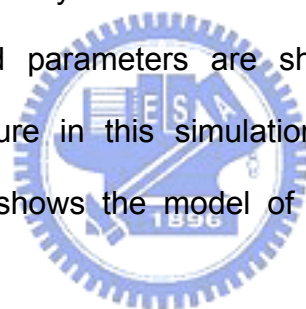
Figure 5-8 shows normalized far-field patterns of the SSFC-LED and CFC-LED under 20 mA current injection, respectively. For detail comparison, the normalized far-field patterns via two directions ((1-106)-plane to (1-102)-plane, X-axis; (11-25)-plane to (11-25)-plane, Y-axis) are measured. It can be observed that the electroluminescence (EL) intensities of SSFC-LEDs is concentrated on the near vertical direction (i.e. about between 70° and 110°). In contrast, EL intensities observed from the SSFC-LED are concentrated on the near horizontal direction (i.e. smaller than 60° or larger than 120°) compared to those of the CFC-LED. Figure 5-9 shows the normalized three-dimensional far-field patterns of SSFC-LEDs and CFC-LEDs, which verifying that the oblique sidewall can vary far-field patterns and lead to larger 50% viewing angles. Such an enhancement could be attributed to the oblique sidewall and thicker window layer that photons can have a larger probability to

be emitted from the device in the near horizontal directions.

5-2.2 Monte-Carlo ray-tracing calculations

In order to investigate the fundamental of enhancement of light output with different etching time of sapphire shaping FC-LEDs. we used the commercial ray-tracing software employing the Monte-Carlo algorithm to obtain trajectory of ray-tracing, enhancement efficiency and spatial intensity distributions of radiometric and photometric data.

The shape and size of the solid model for the ray-tracing calculation is determined and exactly the same as the SEM images and microscopic measurements of the geometry of SSFC-LEDs as shown in figure 5-2 and figure 5-3. The simulated parameters are shown in table 4-1 and the wavelength and temperature in this simulation are 460 nm and 300 K, respectively. Figure 5-10 shows the model of SSFC-LED in the TracePro software.



The solid model is built up with combining the simple solid objects and each semiconductor layers adjoin to the others. Light rays are generated in the active layer with a uniform random distribution. Monochromatic radiation with the peak wavelength of the measured spectral emission (460 nm) is used in the simulation.

Figure 5-11 (a) and (b) shows the candela maps of CFC-LEDs and 100 μm SSFC-LEDs, respectively. The intensity of 100 μm SSFC-LEDs obviously exceeds that of CFC-LEDs and the intensity distribution is the same as normalized far-field patterns of CFC-LEDs and 100 μm SSFC-LEDs as shown in figure 5-9. Therefore, the improved light extraction efficiency can be further supported by the simulation result and the increase of light output power of

SSFC-LEDs can be verified by ray-tracing situations as shown in figure 5-12 because oblique sidewall can reduce photon path length and absorption to lead to enhance light output power.

The output power versus different etching depth of SSFC-LEDs simulating with TracePro software can be obtained from the irradiance maps. Therefore, the enhancement efficiency can be calculated and it is found that the extraction efficiency is increased by larger etching depth of SSFC-LEDs as shown in figure 5-13. The simulated result of 100 μm SSFC-LEDs is similar to experiment performance of 55% and enhancement efficiency gradually converges. According to simulation data, we will employ longer etching time to enhance extraction efficiency of FC-LEDs further in the future.



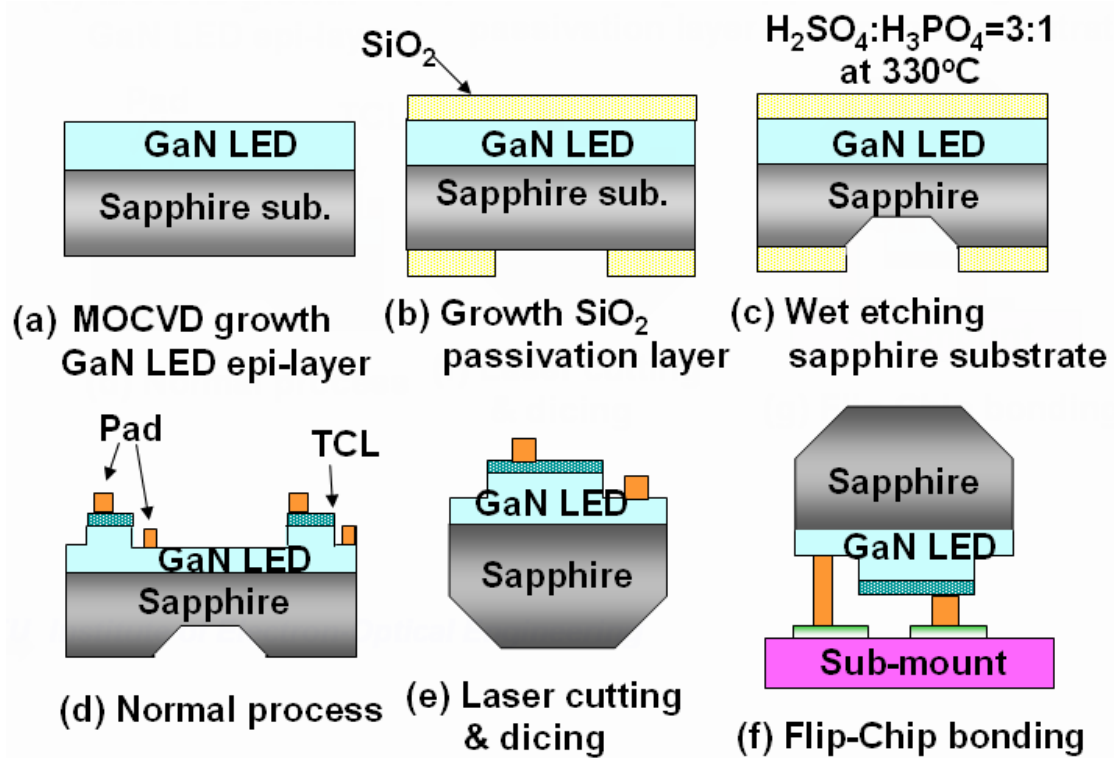


Figure 5-1 Schematic of fabrication steps of sapphire shaping FC-LEDs.

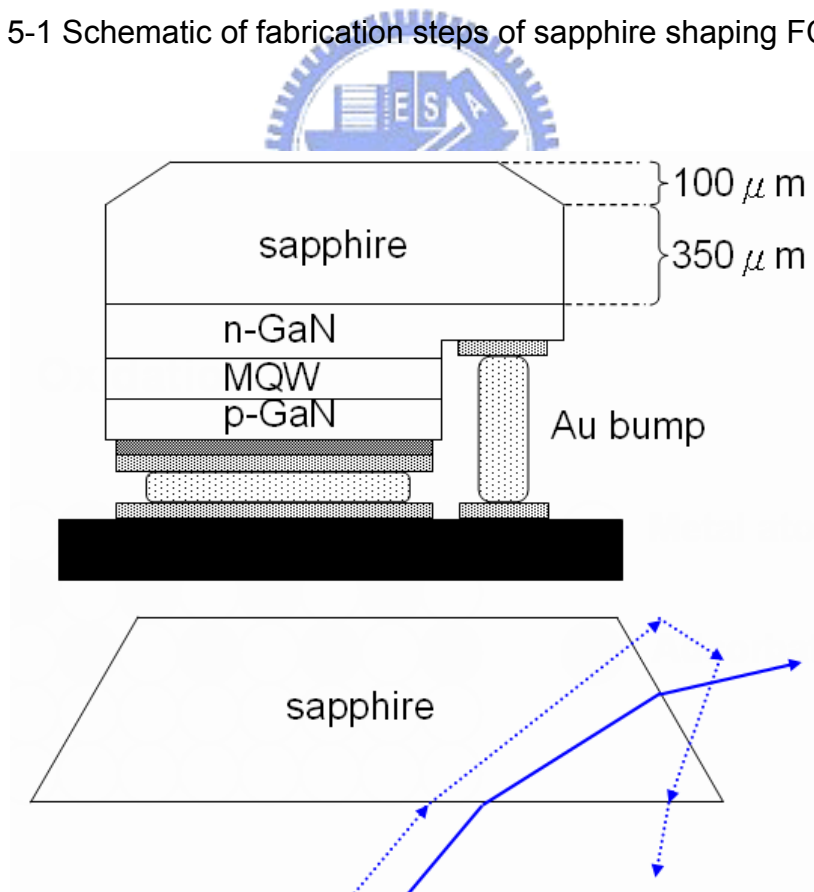
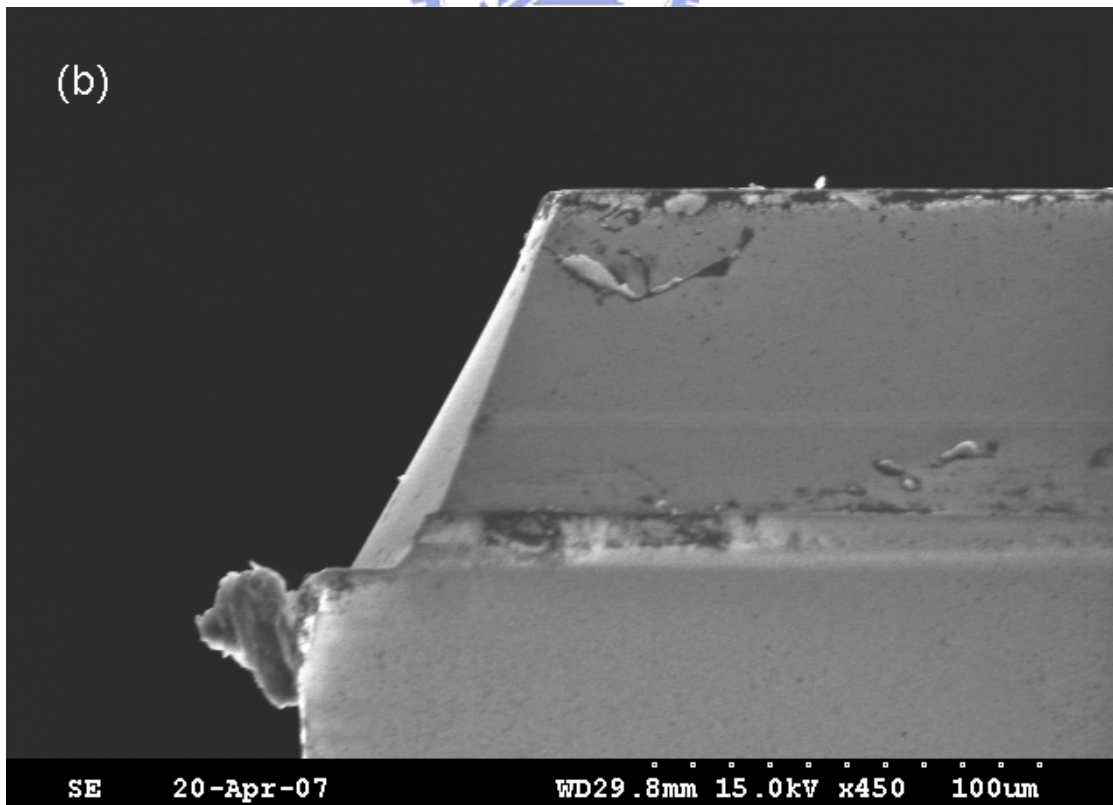
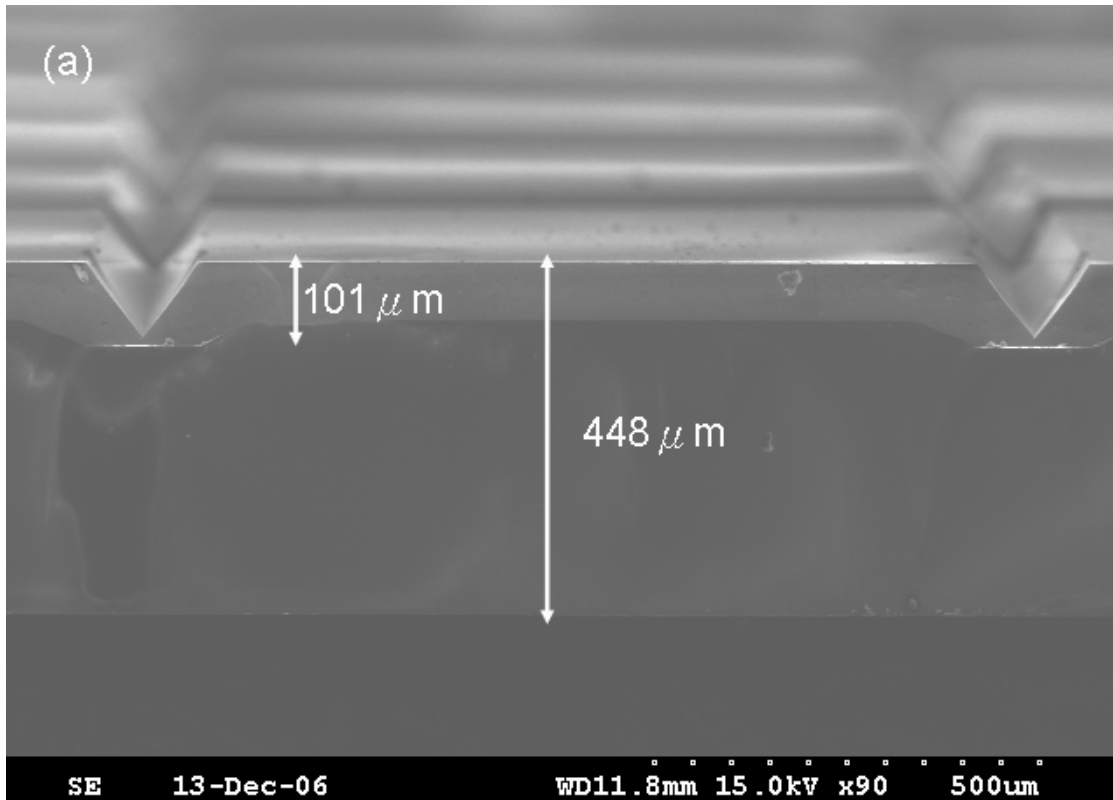


Figure 5-2 Schematic drawing of the GaN SSFC-LEDs, illustrating the means by which light may be extracted from the oblique sapphire sidewall.



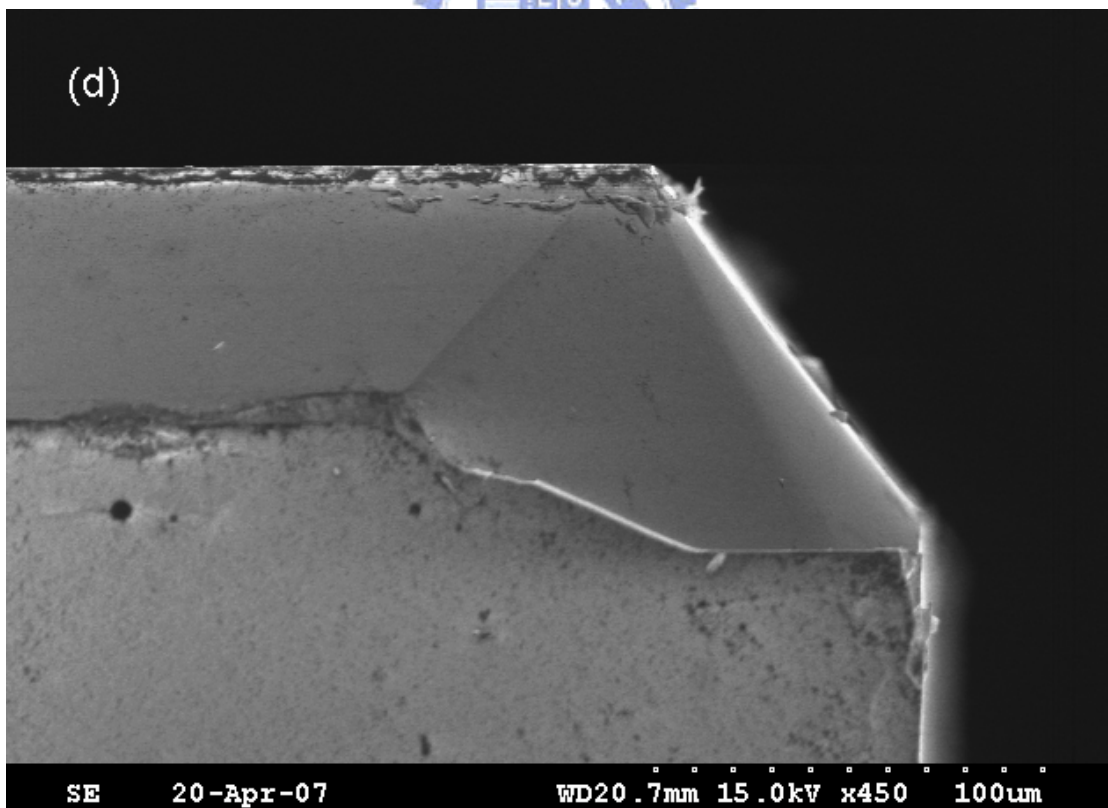
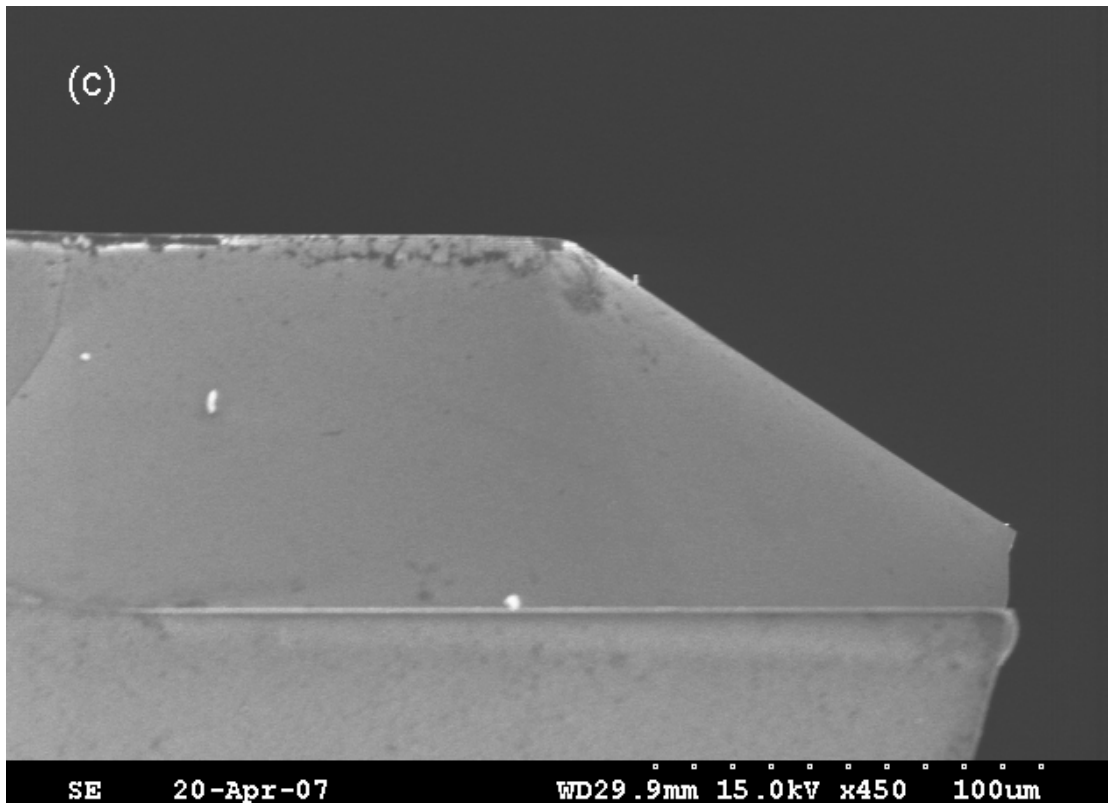


Figure 5-3 SEM images of SSFC-LED. (a) shows the cross view and (b), (c), (d) show the angle of 60°, 30° and 50° against (0001) c-axis, respectively.

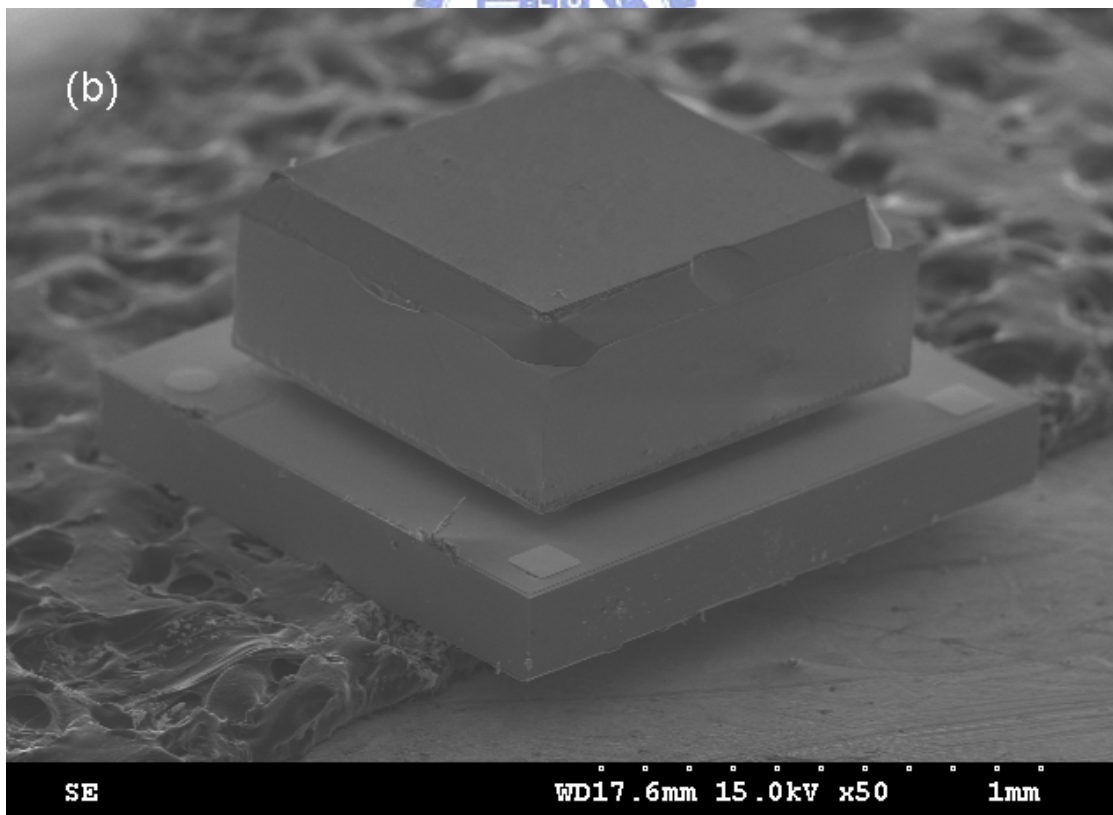
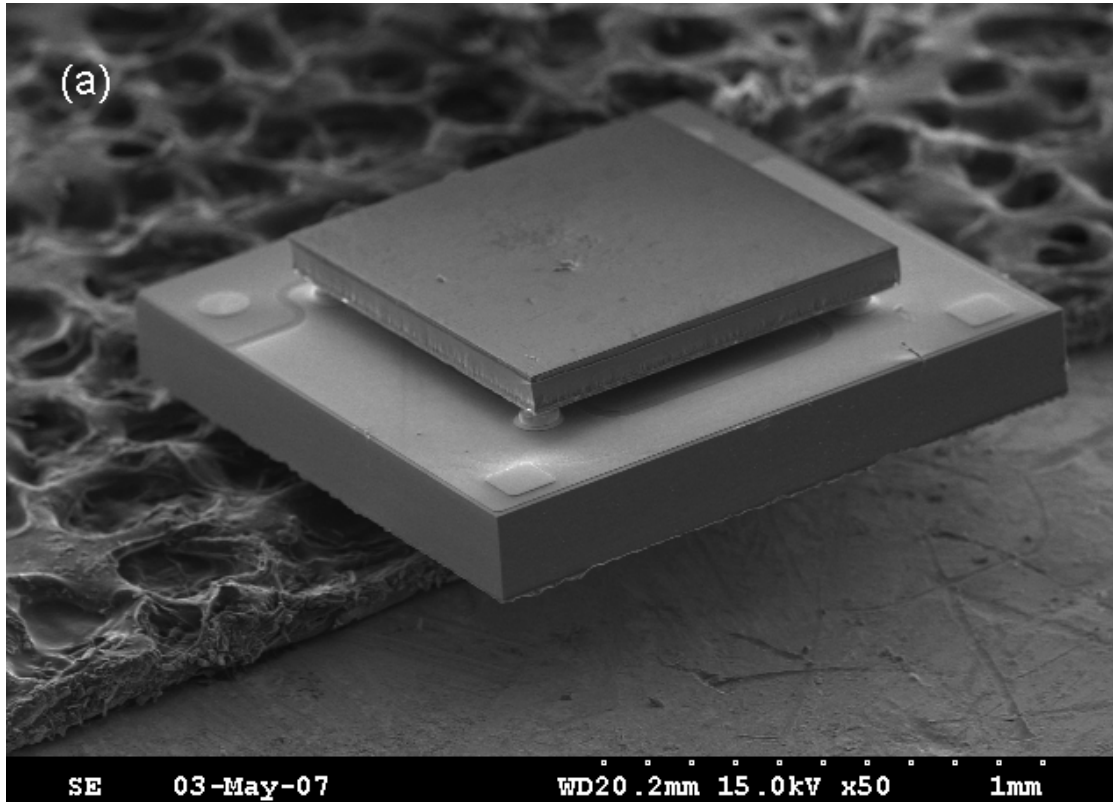


Figure 5-4 Scanning electron micrographs of (a) CFC-LED and (b) SSFC-LED devices.

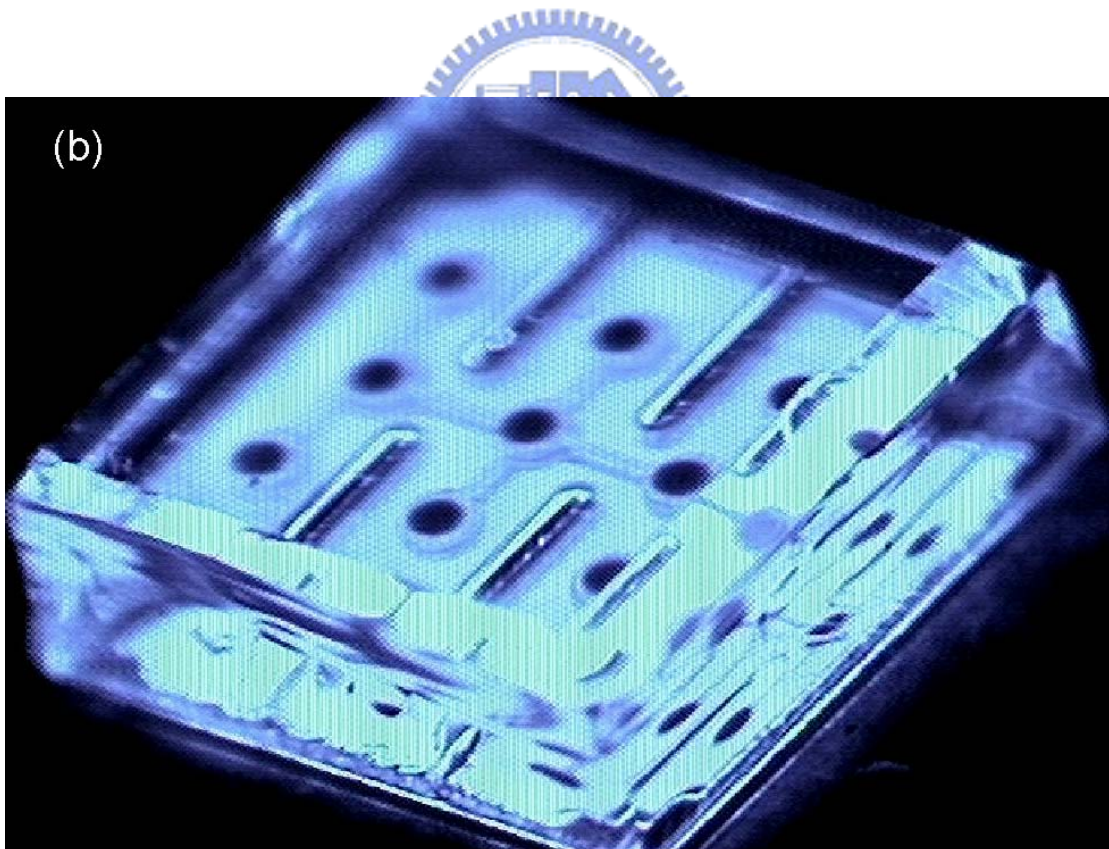
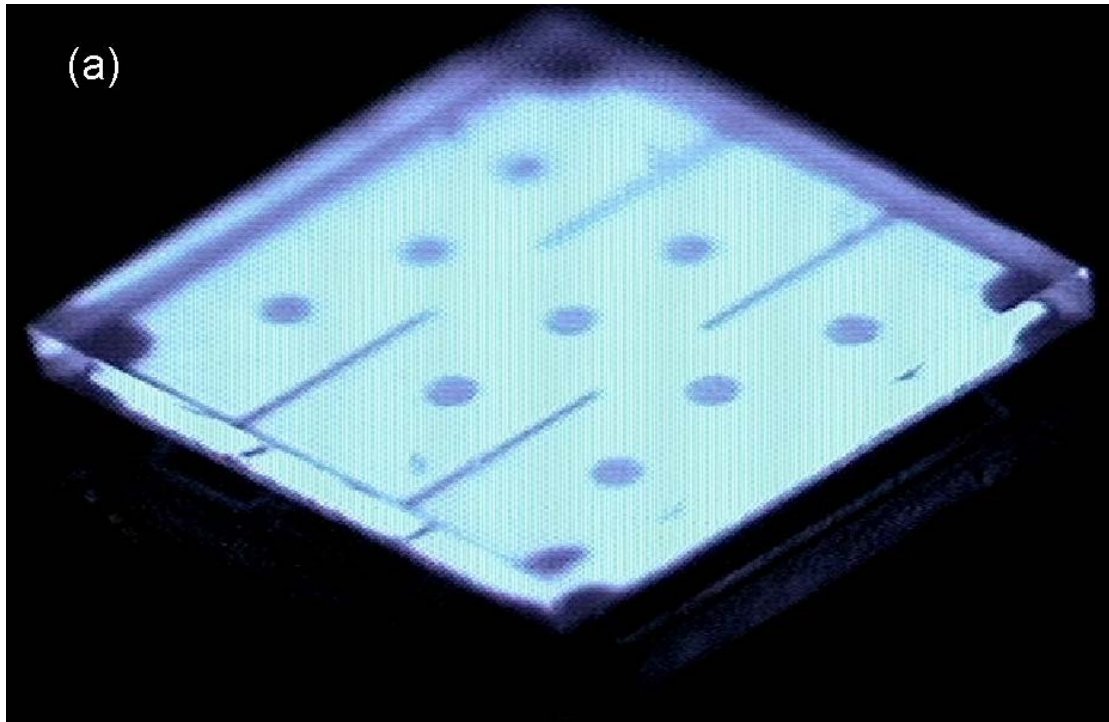


Figure 5-5 Photomicrographs of (a) CFC-LED and (b) SSFC-LED chips (40X40 mil) operating at 20 mA (dc) with an emission wavelength of $\lambda_p \sim 460$ nm.

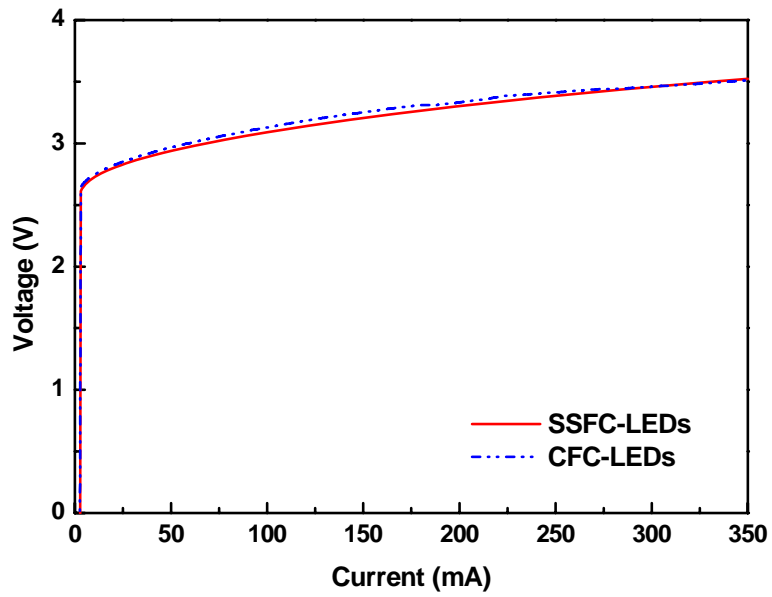


Figure 5-6 The corresponding current-voltage (I-V) characteristics of SSFC-LEDs and CFC-LEDs.

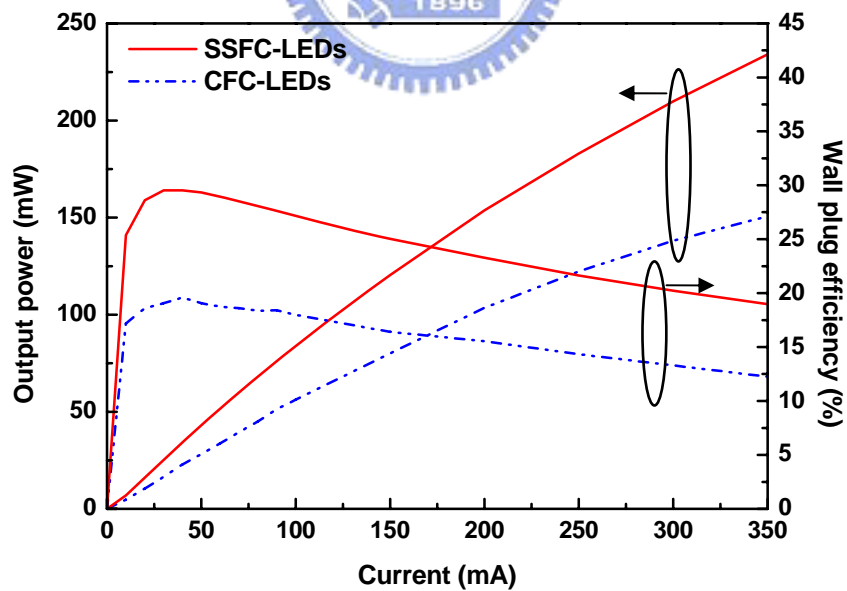


Figure 5-7 The light output power and wall plug efficiency as a function of injection current for $\lambda_p \sim 460$ nm devices of SSFC-LEDs and CFC-LEDs.

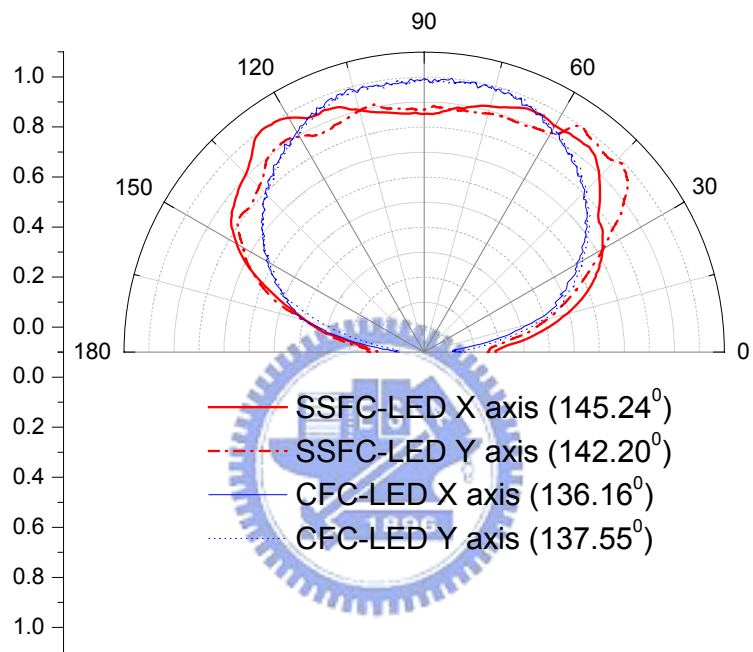


Figure 5-8 The normalized far-field patterns of the SSFC-LED and CFC-LED versus two directions ((1-106)-plane to (1-102)-plane, X-axis; (11-25)-plane to (11-25)-plane, Y-axis), respectively.

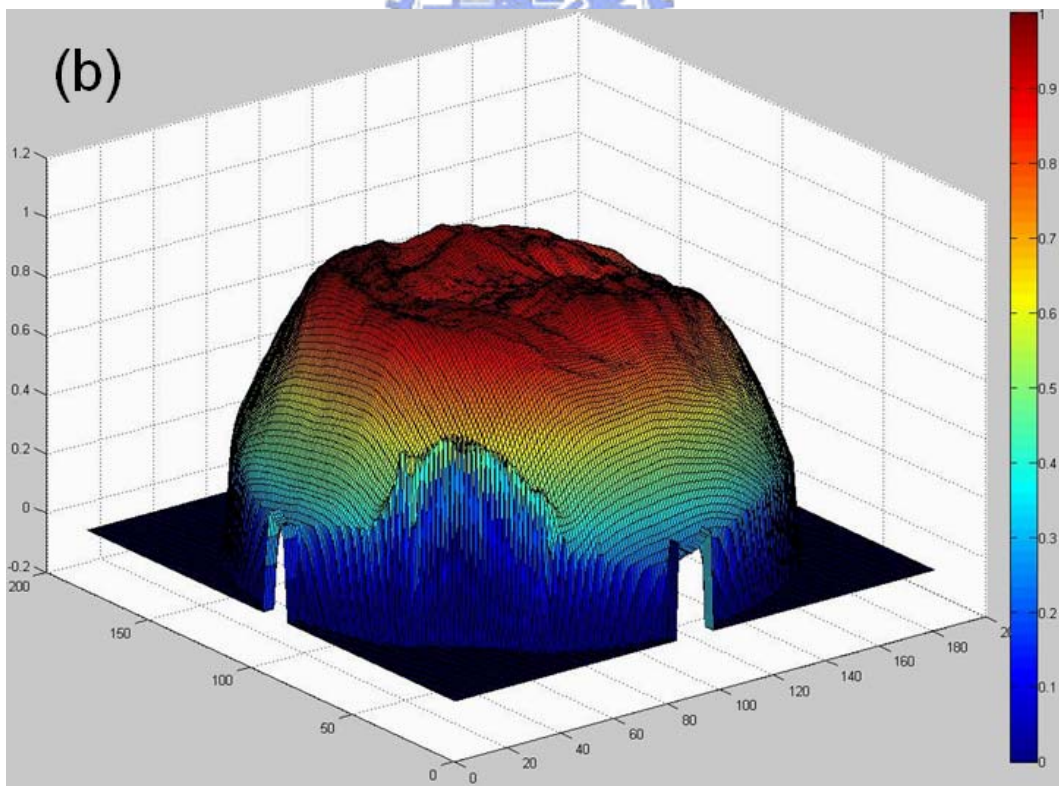
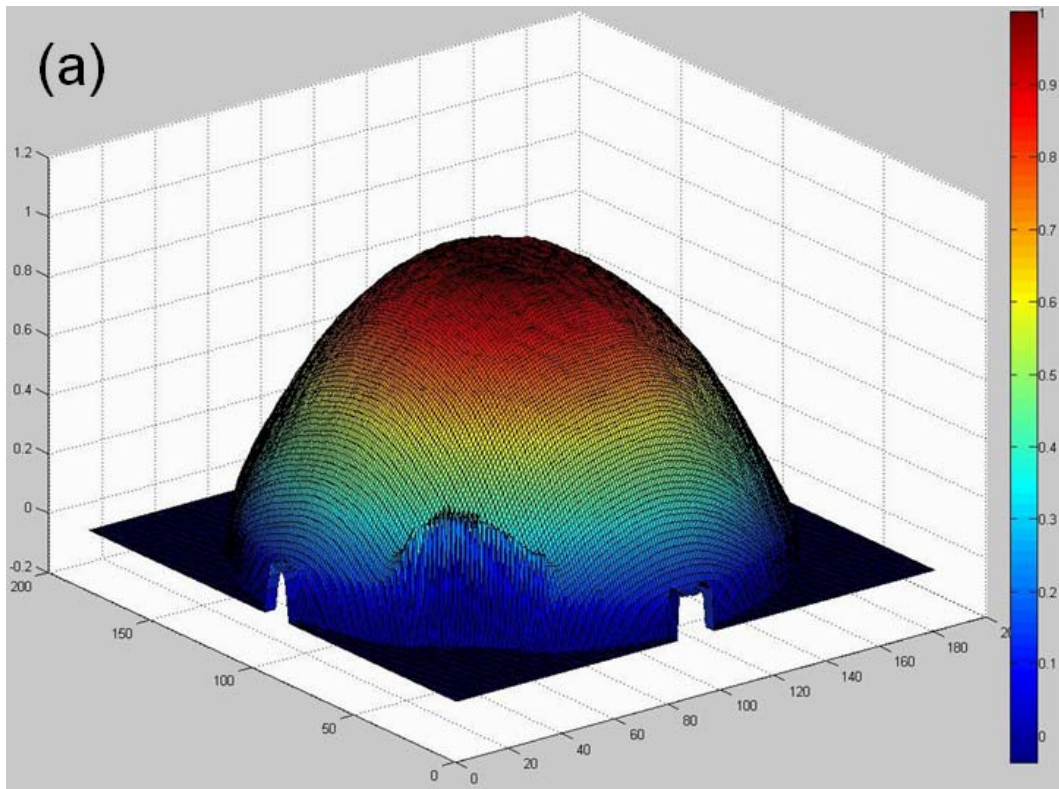


Figure 5-9 The normalized three-dimensional far-field patterns of (a) CFC-LEDs and (b) SSFC-LEDs.

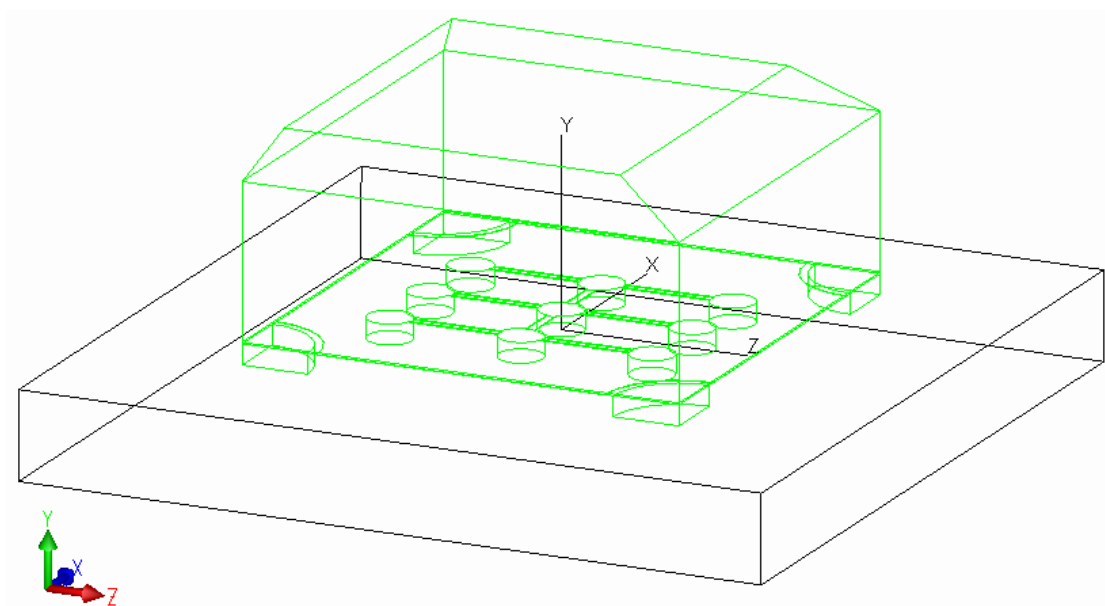


Figure 5-10 The structure of the simulated model in TracePro software.

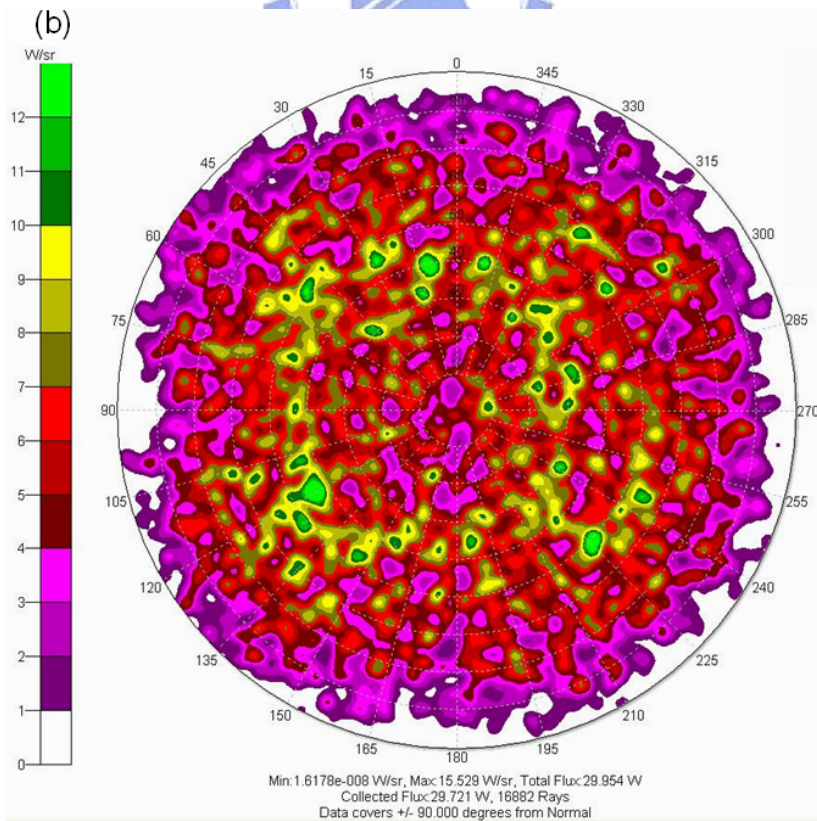
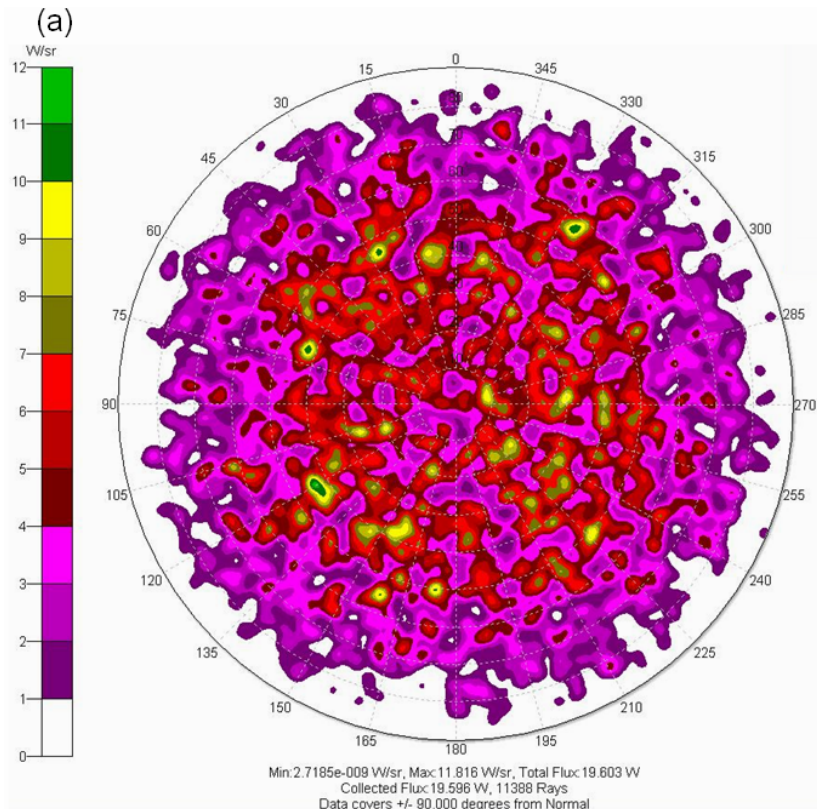
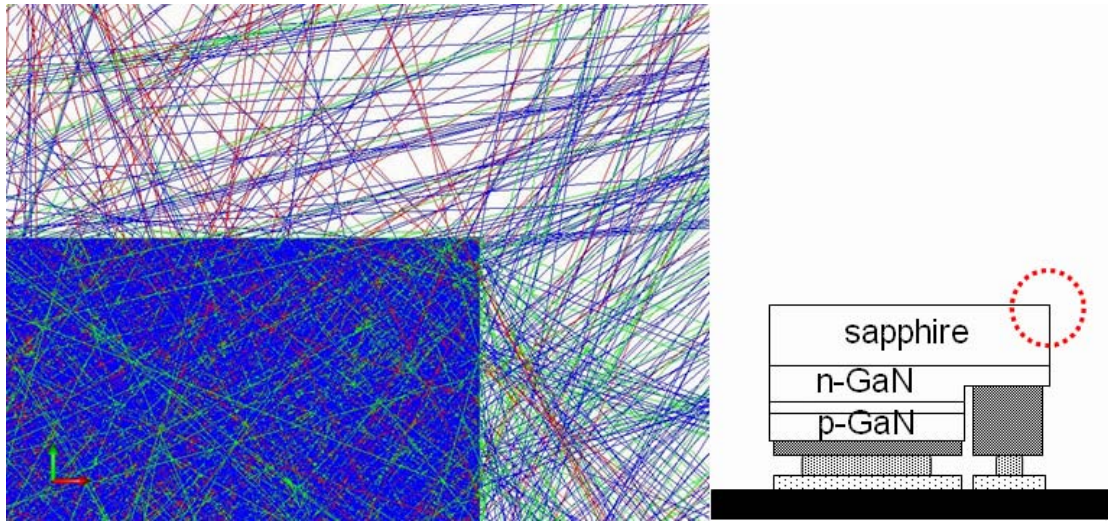


Figure 5-11 The candela maps of (a) CFC-LEDs and (b) 100 μm SSFC-LEDs.

(a)



(b)

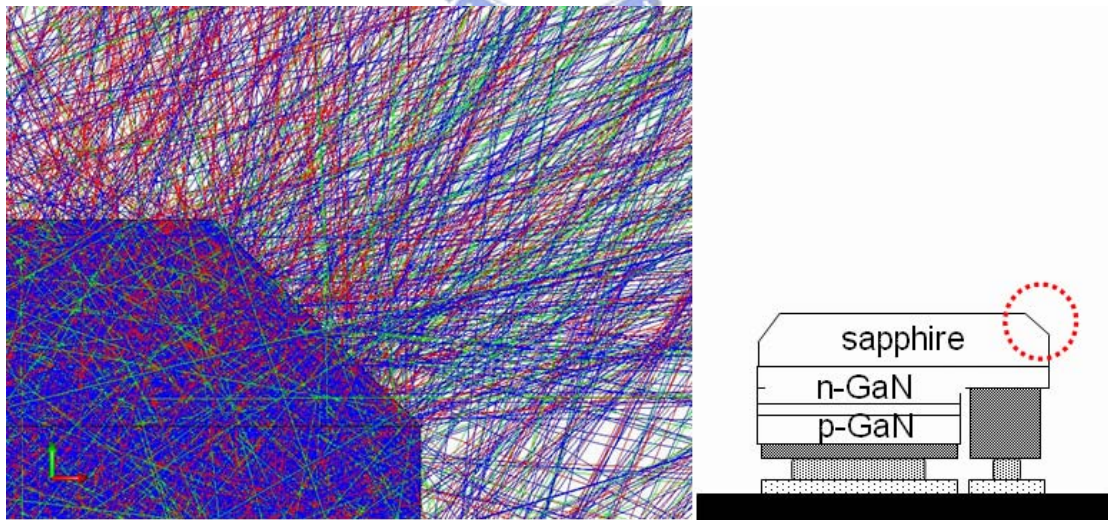


Figure 5-12 The ray-tracing images of oblique sidewall of (a) CFC-LEDs and (b) SSFC-LEDs.

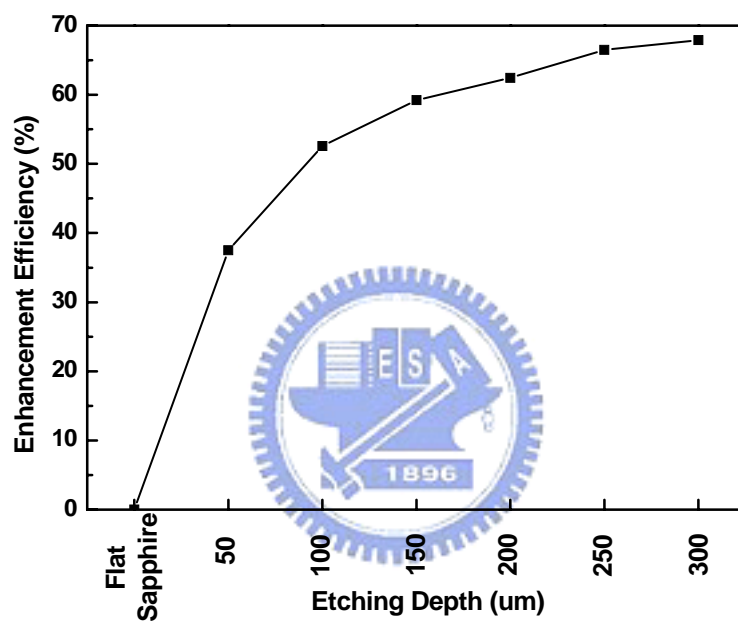


Figure 5-13 The calculated enhancement of the light extraction efficiency with the increasing of etching depth of SSFC-LEDs.